Photo-triggered assembly/disassembly of macroscopically ordered monodomain lamellar structure in side-chain liquid crystalline polymer containing strong polar azobenzene mesogens

Jian Liu[a]; Mingle Wang[a]; Yuanyuan Li[a]; Hejin Zhong[a]

[a] State Key Laboratory Cultivation Base for Nonmetal Composites and Functional Materials, Southwest University of Science and Technology, Mianyang, China

Online publication date: 15 January 2011

PLEASE SCROLL DOWN FOR ARTICLE

Taylor & Francis
Taylor & Francis Group

Photo-triggered assembly/disassembly of macroscopically ordered monodomain lamellar structure in side-chain liquid crystalline polymer containing strong polar azobenzene mesogens

Jian Liu*, Mingle Wang, Yuanyuan Li and Hejin Zhong

State Key Laboratory Cultivation Base for Nonmetal Composites and Functional Materials, Southwest University of Science and Technology, Mianyang, China

Assembly of ordered structures by an external stimulus allows for design of functional materials with enhanced physical and chemical properties. A new side-chain liquid crystal polymer containing strong polar azobenzene mesogens was synthesised. A macroscopically ordered monodomain smectic-like lamellar structure having orientational order and positional order was immediately assembled by linear polarised light irradiation (473 nm, 20 mW/cm^2) at room temperature. The lamellar layer with its periodic *d*-spacing of 1.9 nm and mesogens arranged at an inclination angle of about 75° were characterised by X-ray diffraction and polarising optical microscopy which showed a diffraction peak at $2\theta = 4.53°$ and an off-centred interference figure. Reversible assembly and disassembly of the lamellar phase were achieved by alternative irradiation with polarised light and non-polarised light. Potential factors influencing the assembly of the ordered lamellar structure were investigated by controlling the mesogens out-of-plane orientation and by changing the polarities of mesogens. The difference in arrangement of the mesogens between the lamellar phase and a thermotropic smectic phase was also compared by heating the selectively exposed film. The light controllable assembly of mesogens provides an easy route to assemble a lamellar phase in azobenzene containing polymers for application in optical and photonic devices.

Keywords: azobenzene; assembly; orientation; lamellar; polarity

1. Introduction

Over the last decade, azobenzene containing liquid crystalline polymers (LCP) have attracted significant attention due to their photo-responsive phase transitions for applications as optical and photonic materials [1–4]. There are several types of liquid crystalline states, depending upon the amount of order in the materials. In general, a nematic LC phase has only orientational order but a lamellar smectic phase combines the orientational order with positional order [5]. Therefore, the mesogens in the lamellar smectic phases have more order than that of molecules existing in the nematic phase [6, 7]. The smectic phase can be achieved by a spontaneous self-assembly of mesogens as a result of changing temperature or by dissolving the materials in solution; however, the spontaneously self-assembled smectic phases are composed of random microdomains. It is virtually macroscopically disordered because each microdomain is oriented arbitrarily with respect to its neighbour domain.

More recently, Petchsirivej *et al.* [8] demonstrated that a macroscopically ordered monodomain lamellar phase could be prepared by Langmuir–Blodgett horizontal deposition of a polyacrylate-based side-chain LCP with 4'-(6-acryloxy) hexyloxy-4-methoxyazobenzene as the side chain. In another way, Uekusa *et al.* [9] assembled a monodomain lamellar

phase by adopting surface-initiated atom transfer radical polymerisation of LC polymer brushes bearing an azobenzene mesogenic group in the side chains. The azobenzene mesogens were orientated parallel to the substrate and the smectic layer perpendicular to the substrate plane. Photoinduced assembly of a monodomain lamellar structure was also achieved by Stumpe's group [10]. In their case, linear polarised light (LPL) irradiation of spin-coated smectic main-chain polyester with mesogenic 4, 4'-dioxyazobenzene groups in the backbone and subsequent thermal isomerisation of the azobenzene groups finally established a monodomain of lamellar phase.

Direct light-induced self-assembly of the mesogens into a macroscopically ordered phase is particularly attractive because the process can be remotely controlled, quickly switched and easily focused into specific areas. Motions of azobenzene groups under the effect of a linearly polarised optical field have been extensively investigated in the past 30 years. Although a wide level of mesogen motions have been reported in the literature, the light-triggered self-assembly motion of azobenzene mesogens is still limited [11–13]. The mechanism of azobenzene motion upon LPL irradiation claims that only the molecular long axis perpendicular to the direction of the electric field vector will stop the isomerisation and reorientation

*Corresponding author. Email: jianliu@swust.edu.cn

motion [14–16]. This rule implies that only an orientational order could be obtained upon LPL irradiation, which was widely demonstrated in previous literature in which no positional order of azobenzene mesogens was observed under LPL irradiation [17, 18].

Besides the external factors, many researchers have stressed the importance of the polarity of mesogens on the self-assembly of azobenzene containing LCPs. For example, Canessa *et al.* and other groups [19–22] reported that methacrylate polymers containing strong donor–acceptor substituted azobenzene mesogens typically form smectic phases but none or weakly polar groups substituted azobenzene mesogens form nematic phase instead, which stresses the role of dipole–dipole intermolecular interactions in the growth of the positional order in the smectic phase [23–27]. However, the intermolecular dipole–dipole interaction has been frequently overlooked under the condition of optical field in the literature [2, 28, 29]. Still, the thermotropic self-assembly by annealing occurs at temperature above T_g in the LC mesophase, but the photoinduced assembly process takes place at room temperature. To assemble the mesogens below T_g, a stronger driving force needs to overcome the motion confinement. In this paper, a strongly polar mesogen containing the LCP poly(6-(1-(4-(4-nitrophenylazo)phenyl)piperazino)hexyl) methacrylate (pSDAAB) was synthesised. We might therefore expect that the strong dipole–dipole interactions will provide a strong driving force for the mesogen assembly accompanied by their photoinduced orientation at room temperature [30, 31]. As expected, the mesogens assembled into a monodomain lamellar stack upon LPL irradiation (473 nm, 20 mW/cm^2), which exhibited orientational order and positional order in the pumped film. Nevertheless, an analogously structured side-chain LC polymer bearing weakly polar azobenzene mesogens (pWDAAB) showed only an orientational order under the same light irradiation conditions. Here we report the unique motion and assembly of mesogens producing a lamellar structure upon LPL irradiation in the solid film.

2. Experimental details

2.1 Characterisation

UV-vis absorption spectra were recorded on a Shimadzu UV-2401PC spectrophotometer. Mesogenic textures were observed by a Nikon YS2 polarising optical microscope (POM) equipped with a hot-stage. The thermotropic properties of the polymers were determined with a differential scanning calorimeter (DSC, Perkin–Elmer Priys-1) at a scanning rate of 10°C/min. X-ray diffraction (XRD) patterns were recorded on a Rigaku D/max-rA rotating anode X-ray

diffractometer, using the CuKα radiation line ($\lambda = 0.15418$ nm) with DS = 1°, SS = 0.5°, RS = 0.15 mm, operating at 40 kV and 100 mA. A *2θ* scan mode of XRD was used to determine the spacing of the smectic layers. XRD of the rocking θ scan model and θ–2θ linkage scan modes were used to study the layer orientation. Because of the high background signals of the glass slice in the samples, the XRD curves of the pumped film were obtained from the sample by casting on a silicon wafer and by exposure under the same condition as for the transmittance tests.

2.2 Film preparation

The films were obtained by casting a solution of 5 wt% polymer in N-methyl-2-pyrrolidone (NMP) on the glass slide and the silica wafer for transmittance tests and XRD tests, respectively. Before casting, the glass slide was first soaked in saturated sodium hydroxide solution for 30 min, sequentially cleaned with a supersonic wave in a deionised water and propanol solution for 10 min and dried with N_2 gas flow. Then the substrates were exposed under an infrared lamp for 10 min and the polymer solutions dropped onto the hot surface, keeping the substrates under the infrared lamp to evaporate the solvent. The films were transferred into a vacuum oven and dried at room temperature for 24 h. The film thicknesses were measured to be 100 nm on an atomic force microscope cut-edge profiler.

2.3 Optical setup

The films were covered with a mask to provide a selective exposure zone. A 473 nm continuous wave diode pumped solid-state laser systems was used as the non-polarised light beam, and a polariser was set to obtain the polarised light. The pump beam was expanded to 10 mm in diameter to obtain a homogeneous light intensity over the entire zone to be exposed. Photoinduced orientation of the resulting films was determined using the experimental set-up described in previous literature [32]. Transmittance was measured by placing the sample between two crossed linear polarisers. To achieve maximum signal, the polarisation vector of the pump beam was set to 45° with respect to the polarisation vector of the probe beam. The irradiation light was set to 45° with respect to the film plane and was performed at room temperature unless specified.

3. Results and discussion

3.1 Polarity characterisation

To study the polarity effect on the assembly behaviour, two side-chain LCPs containing different polarity mesogens were synthesised according to a reported
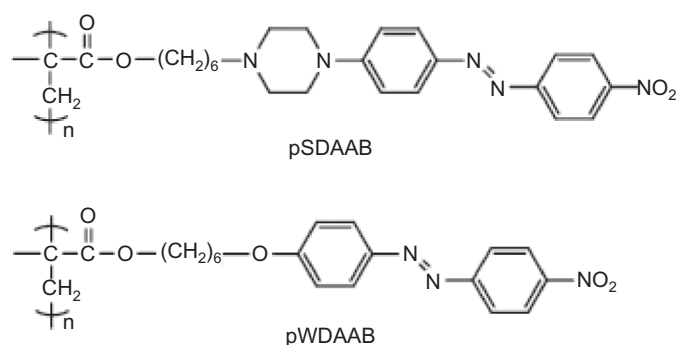
Figure 1. The chemical structures of pSDAAB and pWDAAB.

Table 1. Molecular weight, molecular weight distribution and the liquid crystalline properties of pSDAAB and pWDAAB.

Polymer	M_n	M_w/M_n	Phase transition temperature (°C)	Substitute constants	
				Donor	Acceptor
pSDAAB	4600	1.5	G 62 S 195 I	–N< (–0.83)	–NO$_2$ (0.78)
pWDAAB	7200	1.1	G 52 S 126 I	–O– (–0.27)	–NO$_2$ (0.78)

Notes: G, glassy; S, smectic; I, isotropic.

procedure [32]. As shown in Figure 1, the azobenzene group bonded in pSDAAB is *para*-substituted with strongly polar groups of nitro and piperazino, which has the substitute constants σ (NO$_2$) = 0.78 and σ (N(CH$_2$)$_2$) = −0.83 [27]. By contrast, pWDAAB that substituted with weakly polar groups of -O- group has a donor substitute constant of −0.27 and the acceptor NO$_2$ group as used in pSDAAB (Table 1).

Polymer pWDAAB shows a strong absorption peak around 364 nm and a much weaker absorption peak around 450 nm, corresponding to the absorption of the π–π* transition of the *trans* isomer and the n–π* transition of the *cis* isomer of the azobenzene group (Figure 2(e)). In contrast, the π–π* and n–π* absorption bands of pSDAAB were practically superimposed into a single absorption peak at 446 nm (Figure 2(b)), indicating the strong intramolecular electron donor–acceptor interactions in pSDAAB [33–35]. Moreover, the maximum absorption peak of pSDAAB shows a blue shift at about 70 nm in the solid film compared to that of the solution. In contrast, pWDAAB shows a blue shift of only 42 nm which indicates the stronger dipole–dipole intermolecular interactions of pSDAAB [36–38].

From the DSC results as shown in Figure 3, pWDAAB shows the glass transition at 62°C and the LC to isotropic phase change at 126°C, while pSDAAB shows a broad LC temperature range with glass transition at 52°C and LC to isotropic phase change at 195°C. This result indicates that the strong dipolar interactions in pSDAAB stabilised the liquid crystalline phase. Two polymers exhibit a typical

fan-shaped focal conic smectic texture (as shown in Figure 6(c$_o$)) when annealed from its individual isotropic to LC transition temperature at a cool rate of 10°C/min [39]. Their formations of smectic liquid crystalline phases were also confirmed by XRD measurements in the *2θ* scan mode, which showed a diffraction peak at *2θ* of 3.93° (*d* = 2.2 nm) for pSDAAB and of 3.24° (*d* = 2.7 nm) for pWDAAB (Figure 4). Although the free side-chain length of pSDAAB is longer than that of pWDAAB from calculations with the MM2 simulation, the *d*-spacing of pSDAAB is shorter than that of pWDAAB according to the XRD scanning of the condensate films. These results agree with those obtained by Natansohn's groups that the stronger dipole–dipole forces result in a deeper side-chain interdigitation [18, 40].

3.2 Growth of the monodomain lamellar layer

XRD were used to investigate the formation of the ordered layer structure in pSDAAB film upon LPL irradiation. First it can be seen that the as-cast film exhibits no diffraction peaks in Figure 5(a), indicating the absence of any ordered structure, which is consistent with many previous reports that mesogens were randomly oriented in as-cast film. Upon 5 min of LPL irradiation (20 mW/cm^2) at an incident angle of 45° with respect to the film plane, the pumped film showed a diffraction peak at *2θ* of 4.493° (Figure 5(b)), revealing that a periodic structure was formed [10]. However, the peak intensity of the pumped film was weaker than that of the annealed film (Figure 4(a)), suggesting that
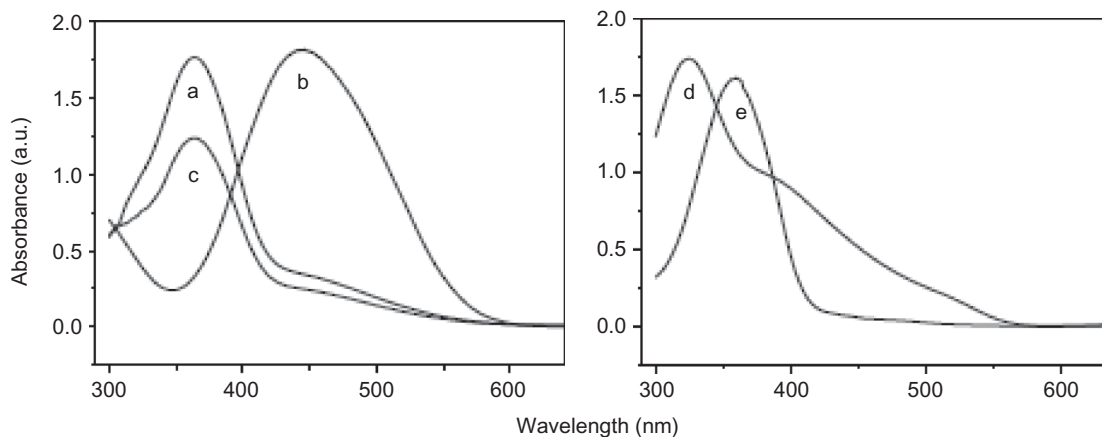
Figure 2. UV-vis absorbance spectra of pSDAAB (a) on an as-cast film, (b) in tetrahydrofuran (THF) solution, (c) on the LPL pumped film (20 mW/cm^2), and of pWDAAB (d) on cast film and (e) in THF solution.
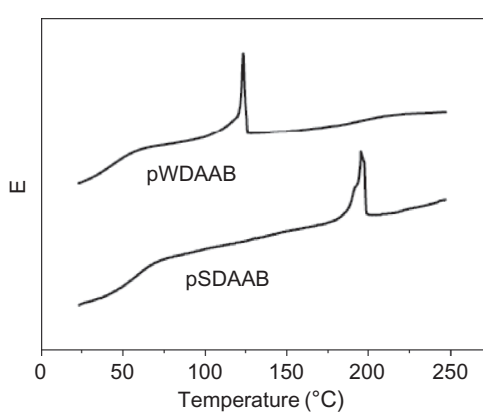

Figure 3. DSC thermograms of pSDAAB and pWDAAB at a heating rate of 10°C/min.
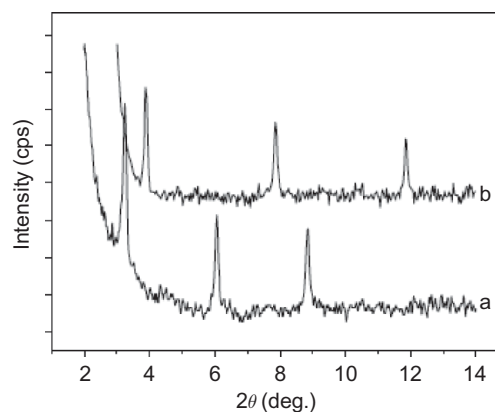

Figure 4. XRD patterns of the thermally induced smectic phase of pSDAAB by annealing from 120°C (a) and pWDAAB by annealing from 100°C (b) at a cooling rate of 10°C/min.
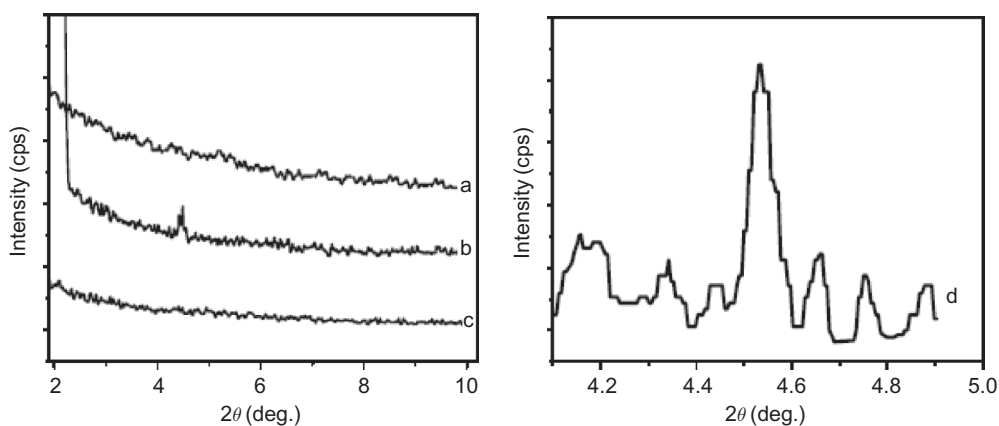

Figure 5. XRD patterns of the *2θ* scan curves of pSDAAB: (a) the as-cast film; (b) the polarised light pumped film (20 mW/cm^2); (c) the non-polarised light pumped film (20 mW/cm^2); (d) *θ–2θ* linkage scan pattern of the LPL pumped film (20 mW/cm^2).

the ordered layers were preferentially orientated [41, 42]. The θ–2θ linkage scan [43, 44] was subsequently performed to substantiate the ordered layer preferred orientation, which yielded a sharp diffraction at $2\theta = 4.53°$ as shown in Figure 5(d), supporting the formation of orientated order layer structure [45]. The peak corresponds to the first-order diffractions arising from the layering distance between sheets of the main chains separated by the mesogens orienting normal to the substrate [41, 46].

Conoscopic observations have been extensively used in elucidating the inclination angle of the optical axis (the molecular long axis) in the literature [47]. To have a better understanding of the mesogen orientation in the lamellar layer, conoscopic images were recorded to characterise the mesogen arrangements. In Figure 6(a_o), the as-cast film shows no birefringence under orthoscopic illumination which suggests that the mesogens were disordered in the film, so no interference image could be observed as seen in Figure 6(a_c). The isotropic nature of the as-cast film is also confirmed by the XRD scanning results of no diffraction signal in Figure 5(a). In contrast, the pumped film (473 nm, 20 mW/cm^2) shows a homogeneous bright field under orthoscopic illumination (Figure 6(b_o)) and a single off-centred black-cross interference figure under conoscopic illumination (Figure 6(b_c)). This suggests a monodomain orientational order was formed upon LPL irradiation and the optical axis of orientated mesogens is inclined with respect to the film plane. As a contrast, the smectic phase (Figure 6(c_o)) of pSDAAB obtained by annealing the as-cast film at 120°C shows a homogenous bright interference figure (Figure 6(c_c)). This is easily understandable considering that the thermally induced smectic phase contains many randomly orientated microdomains, which reflect light averagely in all directions.

3.3 Mechanism for the lamellar assembly

Although the photoinduced growth of the lamellar smectic C like phase differs from previous orientation behaviour in azobenzene containing LCPs exposed under a similar LPL irradiation, the POM observation and the θ–2θ scanning results have directly presented the evidence that a monodomain layer phase was formed and the mesogens were obliquely arranged over the exposed area. Here, a mechanism for the assembly of the lamellar layer phase is illustrated as shown in Figure 7. Initially, the mesogens were randomly distributed in the as-cast film. Upon irradiation, the photoisomerisation broke the mesogen aggregation, and then LPL-guided mesogen orientation motions occurred. It should be emphasised here that the strong dipole–dipole interaction also controls the mesogen motion. Under this situation, the orientation motion induced by LPL cause the mesogen motion perpendicular to the direction of the LPL electric field vector, and the positional motion driven by strong dipolar-dipolar intermolecular interactions also occurred simultaneously, which guides the formation of the lamellar layer. Consequently, a macroscopically ordered monodomain lamellar structure was assembled upon LPL irradiation. As a comparison, Figure 7(c) presents the mesogen distributions in the thermotropic polydomain liquid crystalline phase formed by annealing the polymer at a temperature above the liquid crystalline phase change point, in which the mesogens assembled in randomly oriented smectic domains according to their texture characterisation. In contrast to the strong polar mesogen orientation, the orientation of the weakly polar group substituted azobenzene mesogens in Figure 7(d) was aligned only perpendicular to the polarisation direction. Thus no positional order could be obtained when exposed to a linearly polarised light.
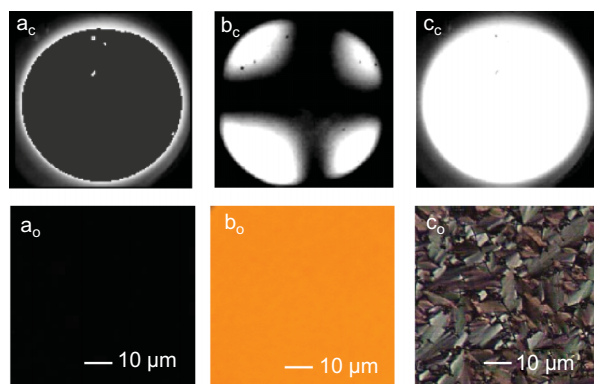

Figure 6. POM observed images under conoscopic illumination (denoted by the sub index c) of pSDAAB: (a) as-cast film, (b) LPL pumped film (20 mW/cm^2), (c) thermally induced polydomain smectic film obtained by annealing at 120°C at a cooling rate of 10°C/min and their corresponding images under orthoscopic illumination (denoted by the sub index o).

3.4 Assembly control
3.4.1 Reversible assembly and disassembly

Assembly and disassembly of the lamellar phase can be triggered by alternate irradiation of the film with LPL and non-LPL at room temperature. When using non-LPL (473 nm, 20 mW/cm^2) irradiation of the lamellar film, the disappearance of the diffraction peak of the film as shown in Figure 5(c) suggests that non-LPL irradiation destroyed the layered order structure. Conoscopic observation on the film confirms the disassembly due to the vanishing of the interface figure in the non-LPL pumped film (Figure 5(a)). In Figure 8,
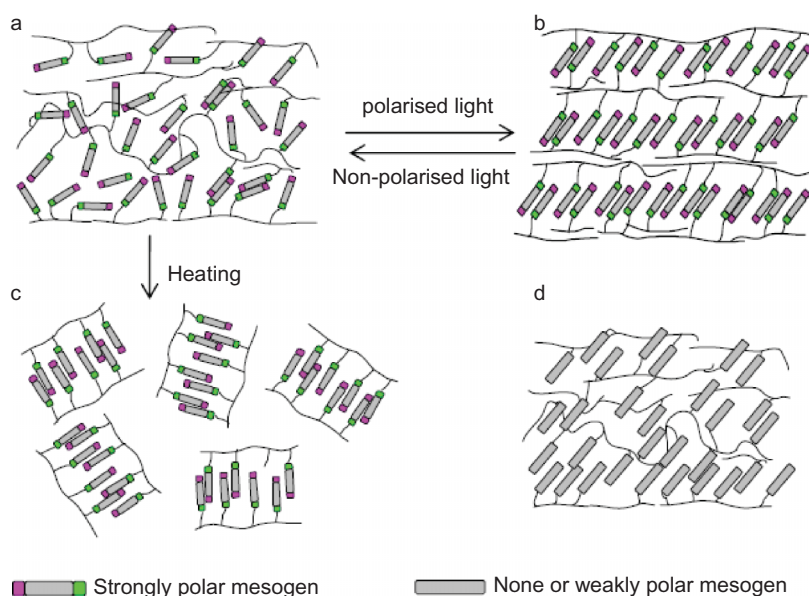
Figure 7. Schematic presentation of the assembly of mesogens: (a) randomly distributed mesogens in the as-cast film; (b) assembly of the lamellar stack upon LPL irradiation of a strongly polar mesogen at room temperature; (c) a thermally induced polydomain smectic phase by heating above T_g; (d) orientation of none or weakly polar mesogens upon LPL irradiation (colour version online).
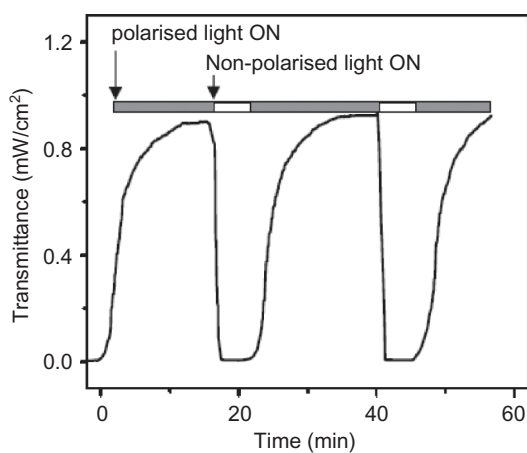

Figure 8. Change in the transmittance as a function of irradiation time upon alternative LPL (473 nm, 20 mW/cm^2) and non-polarised light (473 nm, 20 mW/cm^2).

Figure 9. Change in the transmittance as a function of irradiation time in pSDAAB film. Beam power density: (a) 5 mW/cm^2; (b) 10 mW/cm^2; (c) 20 mW/cm^2; (d) 30 mW/cm^2.

alternate transmittance values changing upon alternate non-polarised light and LPL irradiation present additional evidence of the reversible order–disorder reorientations of the mesogens. In a pump circle, the transmittance increase is a result of the LPL induced assembly, and the transmittance decrease is a result of the disassembly of the order layer upon non-LPL irradiation. However, this decrease in transmittance value is essentially different from the transmittance decrease observed in the orientation curve upon high light intensity irradiation as shown in Figures 9(c) and 9(d), which is a result of the LPL induced out-of-plain orientation [18]. This will be discussed in the next section.
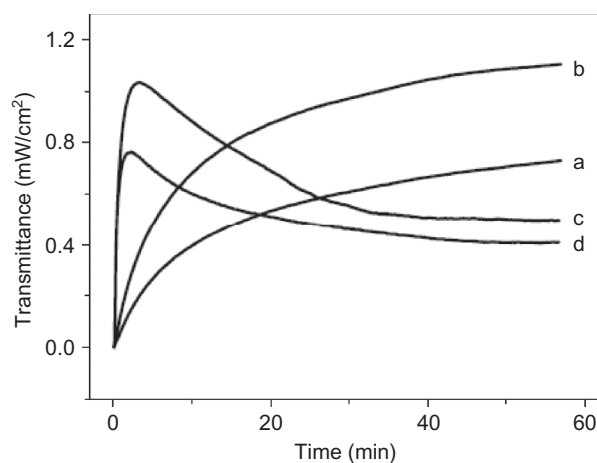
3.4.2 Strong dipole–dipole interaction

From the above analysis, it is quite evident that strong dipole–dipole interactions provide an important driving force for the molecular assembly. For comparison, pWDAAB bearing weak polar mesogens was also conducted upon LPL with 20 mW/cm^2 exposure, and its transmittance value exhibited a similar decrease to that shown in Figure 9(c), which suggests an out-of-plane orientation occurred. However, no diffraction peak was observed (Figure 10(a)) for this pumped pWDAAB film, suggesting the absence of ordered structure. A reasonable explanation is that
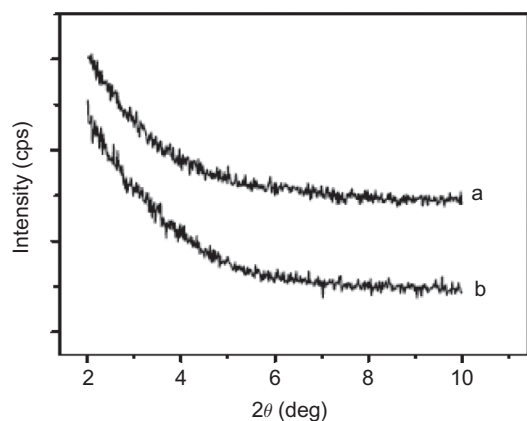
Figure 10. XRD pattern of (a) the pumped pWDAAB film (20 mW/cm^2), (b) the 5 mW/cm^2 power density beam pumped pSDAAB film.

weak polar groups provided a too weak dipole–dipole interaction force to drive the mesogen motion at room temperature.

3.4.3   Out-of-plain orientation

As a contrast to the as-cast film, the decrease of the absorbance intensity in the UV-vis absorbance spectra of the LPL (473 nm, 20 mW/cm^2) pumped film suggests an out-of-plain orientation of the mesogens (Figure 2(c)). This observation is in good agreement with Wu *et al.* [48] as well as our previous reports [32], which claimed that the out-of-plane orientation decreases the absorbance intensity. Furthermore, on the transmittance–irradiation time relationship measurements, previous reports have demonstrated that a decrease in the transmittance value is due to the out-of-plane orientation of the mesogens and the orientation rate exhibits light intensity dependence. Similarly, the decrease in transmittance of pSDAAB in Figure 9 upon high light intensity LPL irradiation (larger than 20 mW/cm^2 in the present case) can be attributed to the LPL induced out-of-plain orientation. In Figure 9(b), the lower light intensity beam (5 mW/cm^2)

pumped pSDAAB film shows no decrease in the transmittance which suggests that the mesogens were orientated in-plane. Correspondingly, this orientated mode produced no layer assembly and was confirmed by XRD results which gave no diffraction peak in the film (Figure 10(b)). This result demonstrates that the out-of-plain orientation plays another crucial role for the assembling of the order lamellar layers. However, the assembly behaviour is inconsistent with the orientation mode of similar structured polymers bearing another type of strong polar mesogen, which were synthesised by Natansohn's group, using ethylamino (denoted as pDR1M) [49] or methylamino (denoted as pXMAN) [18] as the donor groups; the main reason behind this was that the mesogens orientated in the film plane in their system.

3.4.4   Inclination angle of mesogens

As shown in Figure 11, an appropriate LPL pumped pWDAAB film shows a centred conoscopic interference figure upon perpendicular light irradiation and off-centred interference figures upon inclined light irradiation. The interference figure off-centre distance depends on the pump laser oblique angle to the plane of the stage, suggesting the azobenzene mesogens aligned along the propagation direction of the irradiation light. This result is in accord with the report by Ikeda *et al.* of orientation of the mesogens along the propagation direction of the irradiation light, which was controlled by circularly polarised light previously [48] and LPL recently [50]. However, for pSDAAB, the centre of the conoscopic figures (Figure 6(b$_c$)) was not shifted when changing the incident angle of the pump laser. The long axes of the molecules inclined to the plane of the layer at an angle of about 76°, which was calculated by the off-centre distance of the inclination orientated pWDAAB (Figure 12). A more likely interpretation is that the intermolecular interaction governed assembly motion which surpassed the mesogen re-orientation in the light propagation direction.
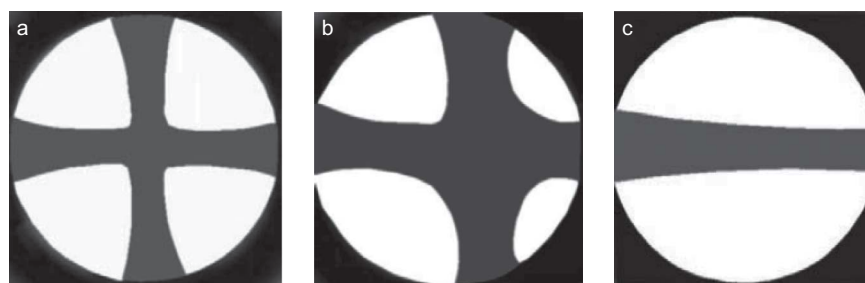

Figure 11.   Conoscopic interference images of pWDAAB as a function of changes in the incident angle (20 mW/cm^2): (a) 90°; (b) 60°; (c) 45°.
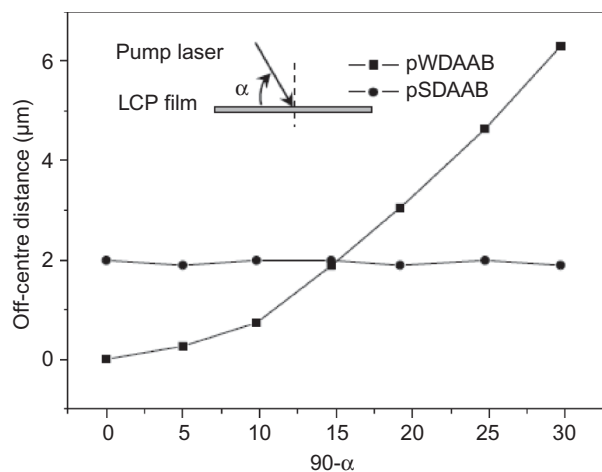
Figure 12. Off-centre displacement distances of the conoscopic interference images as a function of changes in the incident angle (20 mW/cm^2).

3.5 Annealing treatment

The light-triggered growth of the lamellar structure is more than a simple thermotropic self-assembled liquid crystalline smectic structure of a polydomain state. When annealing the selectively exposed pSDAAB film from 190°C, at a temperature below its clear transition temperature, a visible difference between the pumped area and the non-pumped area appeared on the film. In Figure 13(c), the exposed area shows optical transparence whereas the non-exposed area is optically opaque. POM observation reveals that the non-exposed area shows a polydomain smectic texture but the exposed area shows a homogenous bright image (Figure 14). This indicates that the assembled mesogens in the exposed area were

enhanced and preserved the layered structure, which can be attributed to the 'thermal gain-effect' of the liquid crystalline self-organisation processes taking place during annealing. It increases the order of the LC phase when annealed within a temperature range above the glass transition temperature and below the clearing temperature of the liquid crystalline phase [51]. In contrast, the non-exposed mesogens formed a polydomain smectic phase in which light was scattered by the randomly orientated LC domains. This result demonstrates that the strong dipole–dipole interactions stabilised the layer phase [3, 52].

4. Conclusions

For the first time, upon appropriate LPL irradiation of a side-chain liquid crystalline polymer containing strong polarity side-chain mesogens, the macroscopically ordered monodomain lamellar structure was immediately assembled at room temperature. This orientation differs from previous reports due to an accompanied self-assembly occurring during the photoisomerisation and re-orientation process, which results in orientational and positional order in the exposed film. Nevertheless, none or weak polar azobenzene groups used in this work as well as in many previous works showed only a directional motion, which results in only an orientational order in the pumped film. Assembly of an ordered structure by external light stimulus is advantageous because photochemical reactions occur very rapidly and thereby a fast response can be obtained. Besides the strong dipole–dipole interactions, the mesogen out-of-plane orientation and the planar conformation of the mesogens contribute to the layer assembly.
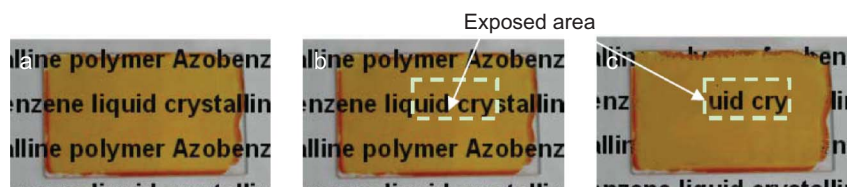

Figure 13. Photograph of pSDAAB: (a) as-cast film; (b) at room temperature selectively exposed film (20 mW/cm^2); (c) after annealing of the exposed film (20 mW/cm^2) at 190°C.
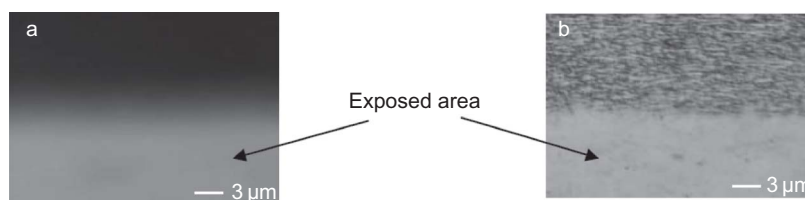

Figure 14. POM images of pSDAAB film: (a) selectively exposed film (20 mW/cm^2); (b) after annealing of the exposed film (20 mW/cm^2) at 190°C.

Acknowledgements

References

[1] Han, J.B.; Yan, D.P.; Shi, W.Y.; Ma, J.; Yan, H.; Wei, M.; Evans, D.C.; Duan, X. *J. Phys. Chem. B* **2010**, *114*, 5678–5685.

[2] Ercole, F.; Davis, T.P.; Evans, R.A. *Polym. Chem.* **2010**, *1*, 37–54.

[3] Natansohn, A.; Rochon, P. *Chem. Rev.* **2002**, *102*, 4139–4175.

[4] Seki, T. *Curr. Opin. Solid State Mat. Sci.* **2006**, *10*, 241–248.

[5] Markun, B.; Zumer, S. *Phys. Rev. E, Stat. Nonlinear. Soft Matter. Phys.* **2006**, *73*, 31702-1-31702-8

[6] Silong, S.; Salisu, A.A.; Rahman, M.Z.A.; Rahman, L.; Ahmad, M. *Am. J. Appl. Sci.* **2009**, *6*, 561–564

[7] Hrozhyk, U.A.; Serak, S.V.; Tabiryan, N.V.; Hoke, L.; Steeves, D.M.; Kimball, B.R. *Opt. Express* **2010**, *18*, 8697–8704.

[8] Petchsirivej, S.; Srikhirin, T.; Bualek-Limcharoen, S.; Kasemjit, P.; Chantarachindawong, R.; Sutapun, B. *Curr. Appl. Phys.* **2008**, *8*, 24–30.

[9] Uekusa, T.; Nagano, S.; Seki, T. *Langmuir* **2007**, *23*, 4642–4645.

[10] Sapich, B.; Vix, A.B.E.; Rabe, J.P.; Stumpe, J. *Macromolecules* **2005**, *38*, 10480–10486.

[11] Shibaev, V.P. *Polym. Sci. Ser. A* **2009**, *51*, 1131–1193.

[12] Kausar, A.; Nagano, H.; Ogata, T.; Nonaka, T.; Kurihara, S. *Angew. Chem. Int. Ed.* **2009**, *48*, 2144–2147.

[13] Yu, H.F.; Asaoka, S.; Shishido, A.; Iyoda, T.; Ikeda, T. *Small* **2007**, *3*, 768–771.

[14] Toshchevikov, V.; Saphiannikova, M.; Heinrich, G. *J. Phys. Chem. B*, **2009**, *113*, 5032–5045.

[15] Bobrovsky, A.Yu.; Pakhomov, A.A.; Zhu, X.-M.; Boiko, N.I.; Shibaev, V.P.; Stumpe, J. *J. Phys. Chem. B*, **2002**, *106*, 540–546.

[16] Kim, M.J.; Lee, J.D.; Chun, C.; Kim, D.Y.; Higuchi, S.; Nakayama, T. *Macromol. Chem. Phys.* **2007**, *208*, 1753–1763.

[17] Tsutsumi, O.; Demachi, Y.; Kanazawa, A.; Shiono, T.; Ikeda, T.; Nagase, Y. *J. Phys. Chem. B* **1998**, *102*, 2869–2874.

[18] Freiberg, S.; Lagugne-Labarthet, F.; Rochon, P.; Natansohn, A. *Macromolecules* **2003**, *36*, 2680–2688.

[19] Canessa, G.S.; Aguilera, C.; Serrano, J.L.; Oriol, L. *J. Polym. Sci. Pol. Chem.* **1996**, *34*, 1465–1473.

[20] Martinez-Ponce, G.; Petrova, T.; Tomova, N.; Dragostinova, V.; Todorov, T.; Nikolova, L. *J. Opt. A-Pure Appl. Opt.* **2004**, *6*, 324–329.

[21] Everaars, M.D.; Marcelis, A.T.M.; Sudholter, E.J.R.; Jerome, B. *Langmuir* **2000**, *16*, 817–823.

[22] Tian, Y.Q.; Xie, J.L.; Wang, C.S.; Zhao, Y.Y.; Fei, H.S. *Polymer* **1999**, *40*, 3835–3841.

[23] Saishoji, A.; Sato, D.; Shishido, A.; Ikeda, T. *Langmuir* **2007**, *23*, 320–326.

[24] Okano, K.; Shishido, A.; Ikeda, T. *Macromolecules* **2006**, *39*, 145–152.

[25] Xu, L.; Suat Hong, G.; Yee Hing, L. *Liq. Cryst.* **2002**, *29*, 675–685.

[26] Li, X.; Goh, S.H.; Lai, Y.H. *Liq. Cryst.* **2002**, *29*, 675–685.

[27] Tsutsumi, O.; Kanazawa, A.; Shiono, T.; Ikeda, T.; Park, L.S. *Phys. Chem. Chem. Phys.* **1999**, *1*, 4219–4224.

[28] Mokdad, A.; Belof, J.L.; Yi, S.W.; Shuler, S.E.; McLaughlin, M.L.; Space, B.; Larsen, R.W. *J. Phys. Chem. A* **2008**, *112*, 8310–8315.

[29] Rau, H. *Photochemistry and Photophysics:* Rabek, J.K., Ed.; CRC Press: Boca Raton, FL, 1990; Vol. 2, p 119.

[30] Qu, S.; Chen, X.F.; Shao, X.; Li, F.; Zhang, H.Y.; Wang, H.T.; Zhang, P.; Yu, Z.X.; Wu, K.; Wang, Y.; Li, M. *J. Mater. Chem.* **2008**, *18*, 3954–3964.

[31] Wang, J.B.; Kulago, A.; Browne, W.R.; Feringa, B. *J. Am. Chem. Soc.* **2010**, *132*, 4191–4196.

[32] Liu, J.; Sun, K.; Li, Z.C.; Gao, J.G.; Su, W.; Yang, J.; Zhang, J.Y.; Wang, P.; Zhang, Q.J. *Polymer* **2004**, *45*, 4331–4336.

[33] Zhu, X.Q.; Liu, J.H.; Liu, Y.X.; Chen, E.Q. *Polymer* **2008**, *49*, 3103–3110.

[34] Zheng, P.J.; Wang, C.; Hu, X.; Tam, K.C.; Li, L. *Macromolecules* **2005**, *38*, 2859–2864.

[35] Wang, H.P.; He, Y.N.; Tuo, X.L.; Wang, X.G. *Macromolecules* **2004**, *37*, 135–146.

[36] Suzuki, I.; Ishizaki, T.; Inoue, H.; Anzai, J. *Macromolecules* **2002**, *35*, 6470–6474.

[37] Freyer, W.; Brete, D.; Schmidt, R.; Gahl, C.; Carley, R.; Weinelt, M. *J. Photochem. Photobiol. A-Chem.* **2009**, *204*, 102–109.

[38] Buwalda, R.T.; Stuart, M.C.A.; Engberts, J. *Langmuir* **2002**, *18*, 6507–6512.

[39] Deng, Y.H.; Li, Y.B.; Wang, X.G. *Macromolecules* **2006**, *39*, 6590–6598.

[40] Labarthet, F.L.; Freiberg, S.; Pellerin, C.; Pezolet, M.; Natansohn, A.; Rochon, P. *Macromolecules* **2000**, *33*, 6815–6823.

[41] Mallia, V.A.; Tamaoki, N. *Mol. Cryst. Liq. Cryst.* **2006**, *454*, 81–90.

[42] Taylor, L.; Richardson, R.M.; Ebbutt, J.; Jones, J.C. *X-ray Diffraction Studies of the Smectic A to Smectic C* Transition within a Surface Stabilised Liquid Crystal Cell*; Gordon and Breach: New York, 1995; pp 255–270.

[43] Kline, R.J.; McGehee, M.D.; Toney, M.F. *Nat. Mater.* **2006**, *5*, 222–228.

[44] Bin Lee, J.; Kwak, S.H.; Kim, H.J. *Thin Solid Films* **2003**, *423*, 262–266.

[45] Birkholz, M. *Thin Film Analysis by X-Ray Scattering*; Betz-druck GmbH: Darmstadt/ Wiley Interscience, 2006.

[46] Liu, N.G.; Chen, Z.; Dunphy, D.R.; Jiang, Y.B.; Assink, R.A.; Brinker, C.J. *Angew. Chem.-Int. Edit.* **2003**, *42*, 1731–1734.

[47] Han, M.; Ichimura, K. *Macromolecules* **2001**, *34*, 82–89.

[48] Wu, Y.L.; Mamiya, J.; Kanazawa, A.; Shiono, T.; Ikeda, T.; Zhang, Q.J. *Macromolecules* **1999**, *32*, 8829–8835.

[49] Cojocariu, C.; Rochon, P. *J. Mater. Chem.* **2004**, *14*, 2909–2916.

[50] Yu, Y.L.; Nakano, M.; Ikeda, T. *Nature (London, UK)* **2003**, *425*, 145.

[51] Stracke, A.; Wendorff, J.H.; Goldmann, D.; Janietz, D.; Stiller, B. *Adv. Mater. (Weinheim, Ger.)* **2000**, *12*, 282–285.

[52] Kerekes, A.; Lorincz, E.; Ramanujam, P.S.; Hvilsted, S. *Opt. Commun.* **2002**, *206*, 57–65.